Analysis of Electromagnetic Characteristics of a Novel Toroidal Acceleration Linear Motor

Zhentian Liu, Qiaopeng Zhou, and Weichao Li

***Abstract*—A high thrust density linear motor, which adopts a novel toroidal structure, applying to load acceleration in confined space is proposed. The basic structure of the toroidal acceleration permanent magnet synchronous linear motor (TA-PMLSM) is depicted, both with its parameters listed. The main characteristics such as air gap magnetic density and electromagnetic thrust are discussed by establishing the electromagnetic field equation in the cylindrical coordinate system. And simulation comparison between the Halbach permanent magnet array and the classical radial one is also made to get a higher density of the magnetic and electromagnetic thrust. Compared with the conventional radial permanent magnet array, results show that the amplitude of back EMF of ring motor under the action of Halbach permanent magnet array has a better sinusoidal, the magnetic density of the air gap increases by 1.3 times, the thrust density increases by 1.42 times, and the main harmonic content of the two referred physical quantity decreases significantly.**

***Index Terms*—Toroidal motor, Linear motor, Electromagnetic field analysis.**

I. Introduction

THE long-straight linear motor is faced with severe problems of suitability when it is used in confined space, such as spaceborne electromagnetic booster, electromagnetic vehicle launch, electromagnetic throwing of small and medium-sized ships, etc. The concept of spiral or ringlike acceleration devices, which can reuse the electromagnetic track and reduce both the characteristic size and cost of the electromagnetic launcher seems to offer a glimmer of hope to alleviate this embarrassment.

The idea of using spiral or ringlike devices to accelerate payload is not just a groundless imagination. Spinlaunch, founded in Long Beach, California in 2015, proposed the concept of a spin ejector putting satellites into orbit by means of rotational acceleration [1]. Similar to the pointer of a clock, as shown in Fig. 1, Spinlaunch uses a vacuum chamber, a rotating hypersonic cantilever, a rotating electric motor, and a bearing gear mechanism to form a centrifuge with a diameter of about 100 meters, which accelerates the payload to rotate for a long time, and then releases it with high-speed and millimeter precision to send the vehicle (as shown in Fig. 2) to the space at the open hatch. The company has raised about $110 million from Airbus, Google, and the U.S. Department of defense in 2020.

Fig. 1. Spinlaunch Vehicle Technical Conceptions.

Fig. 2. Vehicle of Spinlaunch Company.

In this paper, an electromagnetic launch device applied to the confined space is proposed. It adopts an elaborated designed toroidal acceleration permanent magnet synchronous linear motor (TA-PMSLM, shown in Fig. 3) as the power source, other than the way of the rotating motor of the Spinlaunch. TA-PMSLM cancels the intermediate transmission mechanism and has the advantages of direct force, high thrust density, and good controllable performance.

Fig. 3. Profile of the proposed TA-PMSLM.

Manuscript received May 22, 2022; accepted June 14, 2022. date of publication June 25, 2022; date of current version June 18, 2022.

This work was supported in part by the National Key Laboratory Foundation of China under 6142217210505." *(Corresponding Author: Weichao Li)*

Zhentian Liu and Weichao Li are with the National Key Laboratory of Science and Technology on Vessel Integrated Power System, Naval University of Engineering, Wuhan 430000, China. (email: lztxiaoxiao@outlook.com).

Qiaopeng Zhou is with the School of Electrical and Electronic Engineering, Naval University of Engineering, Wuhan 430000, China. (email: 572102327@qq.com).

Digital Object Identifier 10.30941/CESTEMS.2022.00016

Compared with the conventional linear motor, its magnetic field distribution presents the characteristics of staggered medium boundary, multi-harmonic, nonlinear, and multi-form complex magnetic circuit. Its thrust force characteristics are dominated by electromagnetic force, end force, friction force, and centrifugal force together. As an acceleration and launch device, under the background of aperiodic transient high-speed launch and large centrifugal force, how to suppress its thrust fluctuation and improve its thrust density is the core problem of the study of TA-PMLAM.

Previous studies are generally aiming at the long-straight ones. Pan Kailin has established the relationship between several important dimensions of the primary iron core and the end-force, but the analytical method is too complex and the application premise is relatively harsh [2]-[4]. Kinds of literature have published articles to study the key parameter of the winding's inductance to characterize the dynamic characteristics of thrust fluctuation successively [5]-[7]. Xia Jiakuan formulates the dynamic current compensation table of the end effect wave based on the thrust fluctuation curve calculated by the finite element method, and the thrust fluctuation has been significantly reduced [8]. Reference [9] compares and analyzes the structure of the Halbach array without core winding and back iron, as well as the radial one. In [10], a linear synchronous motor based on the Halbach array and high temperature superconducting tape is proposed for the application of the high-speed maglev system.

In this paper, the overview of the proposed TA-PMLSM is shown first in section II. In order to obtain the analytical solutions of magnetic field and electromagnetic force, in section III, the mathematic electromagnetic equations of the TA-PMLSM in the cylindrical coordinate system are deduced. As a further step, a simulation comparison between the Halbach permanent magnet array and the radial one is performed, and the physical quantities of interest are discussed in detail. For that the large thrust and small thrust ripple are both expected for the electromagnetic launcher systems, this paper can provide a basis for the optimum design [11].

II. General View Of The Toroidal Linear Motor

Fig. 4 shows the section structure characteristic of the TA-PMLSM. The primary adopts "back-to-back" three-phase ring winding, the iron core is composed of silicon steel with internal and external slots, the secondary adopts a radial permanent magnet or a Halbach PM array, and the internal and external sides are arranged radially. The linear motor adopts a ring structure connected from head to tail. The centrifugal force is performing intensively during high-speed operation so that the double rotation secondary is adopted in order to balance the payload.

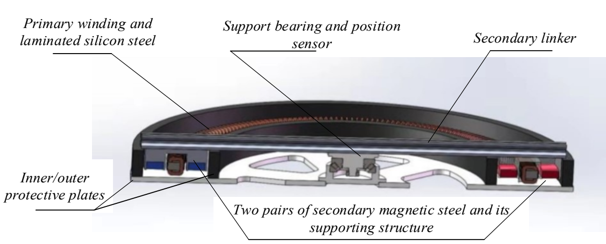

Fig. 4. Section structure of the TA-PMLSM (The motor has two movers, one carrying the payload to be launched and the other carrying a counterweight, so as to counteract the unbalanced centrifugal force).

Fig. 5 shows a designed MAXWELL simulation model of the TA-PMLSM, with 120 slots and 80 poles, and the motor's main parameters designed are shown in Table 1. The permanent magnet array is arranged on both sides of the secondary. The type of the permanent magnet array may be a traditional radial one or a Halbach one. A bilateral Halbach permanent magnet array with its magnetization direction is shown in Figure 6.

TABLE I
PARAMETER OF THE TA-PMLSM

Symbol	Quantity	Values
Q	Number of slots	120
B_{slot}	Slot width	7mm
H_{slot}	Depth of slot	13.3mm
p	Number of poles	40
τ	Pole pitch	21.8mm
D_1	Internal diameter of iron core	500mm
D_2	Outer diameter of iron core	600mm
W_{pm}	Width of Halbach array	85.4mm(Avg)
H_{pm}	Thickness of Halbach array	15mm
P_1	Number of	8
δ	Width of air gap	5mm
L_{ef}	Axial length	30mm

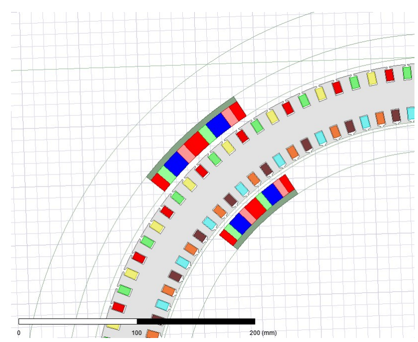

Fig. 5. MAXWELL model of the TA-PMLSM (Partial graph).

Outer Halbach

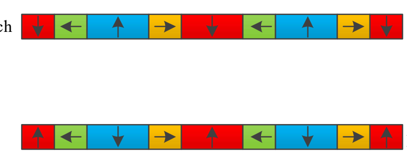

Internal Halbach

Fig. 6. Bilateral Halbach PM array with its magnetization direction.

III. Mathematic Equations Of Electromagnetic Field

The fundamental component of air-gap flux density determines the thrust density. While the air-gap flux density of the permanent magnet motor is mainly generated by the permanent magnet array. Therefore, it is necessary to discuss the magnetic field and force characteristics of different forms of permanent magnet arrays.

Due to the structure of the TA-PMLSM, it is equivalent to two single-side slotted cores placed back-to-back. For simplicity, only a quarter of the motor are analyzed in the following discussion. As shown in Fig.7, a two-dimensional layered model is established. The model is divided into five regions from top to bottom, in which region I is the winding-core region, region II is the air gap region, region III is the permanent magnet array region, region IV is the supporting back iron region, and region V is the infinite region. The interfaces of each area, *a, b, c, d, e,* and *f* have been marked in the figure.

To establish a cylindrical coordinate system, the concentric circle point is seen as the origin point, the direction perpendicular to the paper surface is the *z*-axis, the radial direction is defined as the *r*-axis, and the radius tangential direction is the θ direction.

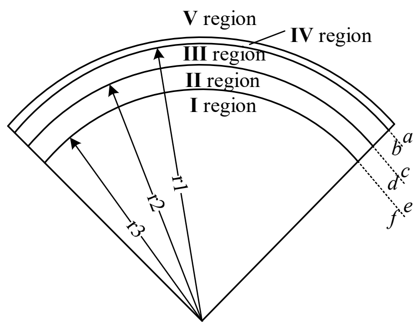

Fig. 7. Two-dimensional layered analytical model of the TA-PMLSM.

A. Magnetic flux density of the air gap region

For the two-dimensional layered model of the motor, the interface conditions of the region II in the upper half-plane (i.e., only a quarter of the motor is considered) can be written as:

$$\begin{cases} \tilde{A}_{zn}^{c}\Big|_{r=r_2} = \tilde{A}_{zn}^{d}\Big|_{r=r_2} = C_1 r_2^{|k_n|} + C_2 r_2^{-|k_n|} + \dfrac{j\mu_0 k_n \tilde{M}_{rn}}{k_n^{\ 2}-1} r_2 \\ \dfrac{\partial \tilde{A}_{zn}^{b}}{\partial r}\Bigg|_{r=r_1} = 0 \\ \dfrac{\partial \tilde{A}_{zn}^{c}}{\partial r}\Bigg|_{r=r_2} - \dfrac{\partial \tilde{A}_{zn}^{d}}{\partial r}\Bigg|_{r=r_2} = -\mu_0 \tilde{M}_{\theta n} \\ \dfrac{\partial \tilde{A}_{zn}^{d}}{\partial r}\Bigg|_{r=r_3} = 0 \end{cases} \tag{1}$$

where C_1 and C_2 are the undetermined coefficients of the Poisson equations about magnetization *M*.

And, $k_n = 2n\pi/\lambda$, λ represents the position angle corresponding to an electric period. $\tilde{M}_{\theta n}$、$\tilde{M}_{rn}$、$\tilde{A}_{zn}$ are the Fourier constants, which are deduced as follows.

There is only a Z-direction component in the solution area of vector magnetic potential, which is a two-dimensional parallel plane field. The permanent magnet is periodically distributed along the inner and outer radius, and the magnetization *M* is Fourier decomposed as:

$$M = \sum_{n=-\infty}^{\infty} \left(\tilde{M}_{\theta n} e^{-jk_n\theta} \hat{i}_\theta + \tilde{M}_{rn} e^{-jk_n\theta} \hat{i}_r \right) \tag{2}$$

$$A = \sum_{n=-\infty}^{\infty} \tilde{A}_{zn} e^{-jk_n\theta} \hat{i}_z \tag{3}$$

where the distribution law and magnetic field intensity of M and A are determined by the type of permanent magnet array.

Then the magnetic field analysis of the permanent magnet array is transformed into the solution of the Fourier constants. Combined with the full solution of the differential equation satisfied by the magnetic vector potential and the first and second boundary conditions of the two-dimensional layered model, the analytical solution of the permanent magnet array is obtained as follows:

$$\tilde{A}_{zn}^{II} = C_3 r^{|k_n|} + C_4 r^{-|k_n|} \tag{4}$$

where C_3 and C_4 are the coefficients of the Laplace equation determined by boundary conditions, which can be explicitly expressed as equation (5). The difference between the Halbach PM array and the counterpart radial one is that the $\tilde{M}_{\theta n}$ in (5) of the later type is equal to zero.

Using the equations above, the magnetic flux density and its radial and axial components in the air gap region are obtained:

$$B^{II}\Big|_{r_3 \langle r \langle r_2} = B_r^{II}\hat{i}_r + B_\theta^{II}\hat{i}_\theta = \nabla \times A^{II} \tag{6}$$

$$B_r^{II}\Big|_{r_3 \langle r \langle r_2} = \sum_{n=-\infty}^{\infty} -jk_n \left(C_3 r^{|k_n|} + C_4 r^{-|k_n|} \right) e^{-jk_n\theta} \hat{i}_r \tag{7}$$

$$B_\theta^{II}\Big|_{r_3 \langle r \langle r_2} = \sum_{n=-\infty}^{\infty} -r|k_n| \left(C_3 r^{|k_n|} - C_4 r^{-|k_n|} \right) e^{-jk_n\theta} \hat{i}_\theta \tag{8}$$

$$C_3 = \frac{\left[\left(\dfrac{r_2}{r_1}\right)^{-2|k_n|} - \left(|k_n|-1\right)\right] \dfrac{j\mu_0 k_n \tilde{M}_{rn}}{k_n^{\ 2}-1} + \left[\left(\dfrac{r_2}{r_1}\right)^{-2|k_n|} + 1\right]\mu_0 \tilde{M}_{\theta n} - 2\left(\dfrac{r_2}{r_1}\right)^{-|k_n|-1}}{r_1^{\ 2|k_n|} - r_3^{\ 2|k_n|}}, \quad C_4 = r_3^{\ 2|k_n|} C_3 \tag{5}$$

B. Electromagnetic force

Maxwell stress tensor method has high analytical accuracy, so this paper chooses the Maxwell stress tensor method to analyze the thrust characteristics. The traction force generated by the two secondaries are derived as equation (9) and (10).

$$F_{em1} = -\mu_0 \lambda l \sum_{n=-\infty}^{\infty} \left(\tilde{H}_{rn}\Big|_{r=r_2} e^{-jk_n\theta} \right)\left(\tilde{H}_{\theta n}\Big|_{r=r2} e^{-jk_n\theta} \right) \tag{9}$$

$$F_{em2} = -\mu_0 \lambda l \sum_{n=-\infty}^{\infty} \left(\tilde{H}_{rn}\Big|_{r=r_3} e^{-jk_n\theta} \right)\left(\tilde{H}_{\theta n}\Big|_{r=r3} e^{-jk_n\theta} \right) \tag{10}$$

where *l* is the axial length of the effective side of motor windings.

Then, the expressions of the total electromagnetic thrust force is obtained:

$$F_{em} = F_{em1} + F_{em2} \tag{11}$$

An important performance index of the confined space launch device is the thrust density, which could be calculated as:

$$\rho_{Fe} = \frac{F_{em}}{\pi r_1^2 l} \tag{12}$$

IV. Simulation Results

In order to verify the correctness of the analytical equation and lay a foundation for the optimal design, a MATLAB simulation program is compiled, and a finite element MAXWELL model is established.

The simulation comparison between the Halbach permanent magnet array and the classical radial one is made to see how to get a higher magnetic density and electromagnetic thrust, as shown in Fig. 8 and Fig. 9. It is obvious that the finite element results and the analytical calculation results are basically in coincidence, which proves the accuracy of theoretical calculation. The comparison of the air gap flux density *Br* amplitude in two different cases proves that Halbach can enhance the air gap flux density (the fundamental wave amplitude of Halbach type air gap flux density is 1.3 times that of the counterpart one), and the harmonic content decreases greatly (6.11% vs 12.7%), and especially the third harmonic is eliminated.

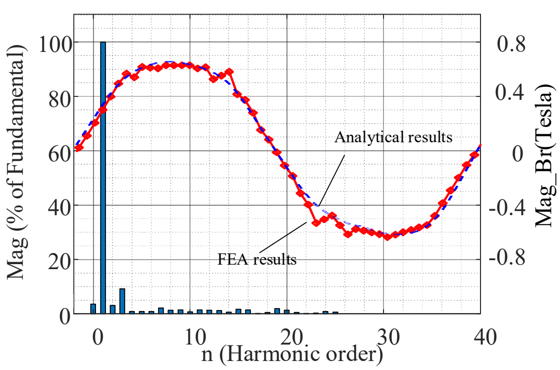

Fig. 8. Air gap magnetic density and the harmonic analysis of the radial permanent magnet array.

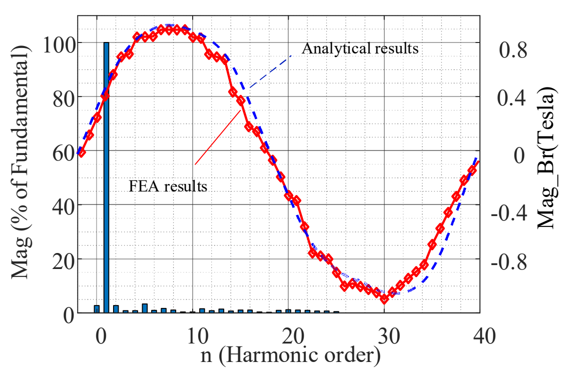

Fig. 9. Air gap magnetic density and the harmonic analysis of the Halbach permanent magnet array.

In a further finite element simulation, the three-phase current rating is set to 50A. In terms of electromagnetic thrust force, it can be seen from Fig.10 that given the same design parameters, the amplitude of the electromagnetic force in the Halbach form is 1.42 times higher than that in the traditional radial one. And the harmonic content has also decreased significantly, especially the third harmonic.

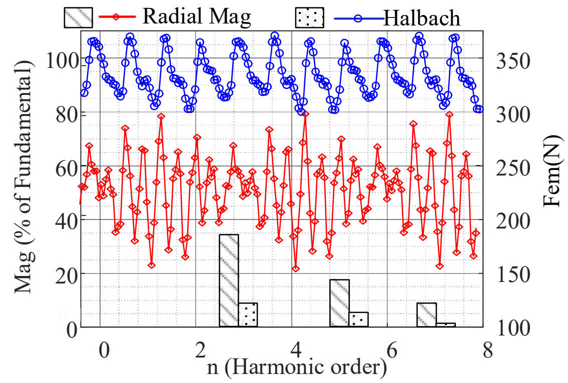

Fig. 10. Comparison of electromagnetic force and harmonic in two cases.

On the other hand, the sinusoidal degree of the back EMF waveform is one of the important indexes of motor design. As can be seen from Fig.11, the two forms of motor back EMF have better sinusoidally. However, owes to its high magnetic induction amplitude of air gap magnetic field, the Halbach form has a high amplitude of its back EMF.

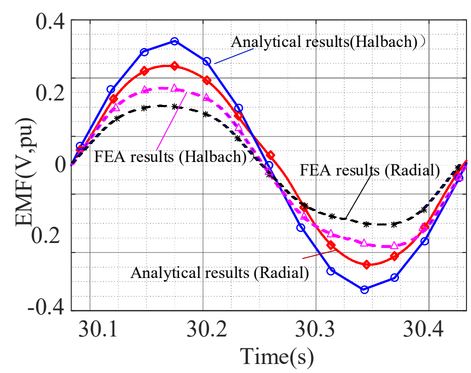

Fig. 11. Comparison of back EMF waveforms in two cases.

Under different quadrature axis current inputs, the thrust density is calculated according to equation (12) and then the curve is fitted in Fig.12. The measured thrust constant of the Halbach array one is 1.1 times that of the radial array motor. The reasons why the measured value of finite element simulation is small than the analytical solution is mainly due to demagnetization of the permanent magnet during the fabrication of the permanent magnet array, neglect of end magnetic leakage in the analytical calculation, and so on.

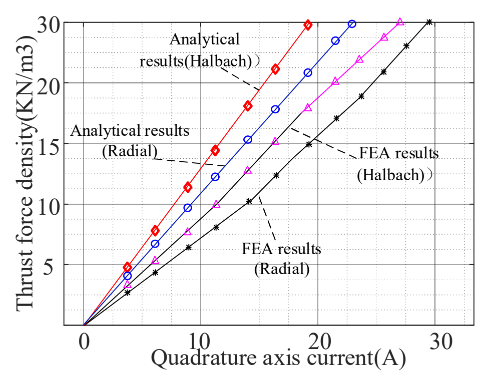

Fig. 12. Comparison of thrust force density waveforms in two cases.

V. Conclusions

This paper focuses on the magnetic-force characteristic analysis and thrust performance optimization of the toroidal acceleration linear motor for electromagnetic launchers in confined space. Simulation results demonstrate that the selection of the Halbach permanent magnet array could obtain a high density of air-gap magnetic and electromagnetic thrust, the third harmonic contents decreased obviously at the same time. This subject aims to explore the physical characteristics and performance optimization of the new motor and lay a foundation for the design and development of electromagnetic launch systems with high thrust density, high launch efficiency, and low launch cost in confined space. The research results of this subject have important basic theoretical guiding significance for enriching the electromagnetic launch methods.

References

[1] Wang. Huanhuan, Chen. Anhong, and Chen. Lin, etc, "Analysis of the Spinlaunched Vehicle Technical Conceptions," *Missiles and Space Vehicles,* vol. 377, no. 6, pp. 78–63, 2020.

[2] Pan Kailin, Fu Jianzhong, Chen Zichen. "Detent force analysis and reduction of PMLSM," *Proceedings of the CSEE*, vol. 24, no.4, pp. 112-115, 2004.

[3] Zhang Ying, "Research on the analysis of detent force and control strategies of permanent magnetic synchronous linear motors", Ph.D. dissertation, Huazhong Univ., Wuhan, China, 2008.

[4] Cheng Yuanxiong, "Study on optima design of thrust ripple of permanent magnetic synchronous linear motors", Ph.D. dissertation, Huazhong Univ., Wuhan, China, 2011.

[5] Li Liyi, Ma Mingna, Liu Jiaxi. "Inductance analysis in pass-through section for multi-segmented permanent magnet linear motors based on magnetic energy perturbation," *Transactions of China Electrotechnical Society*, vol. 28, no. 7, pp. 46-55, 2013.

[6] Liu Chengying, Wang Hao, Zhang Zhijing, et al. "Research on thrust characteristics in permanent magnet linear synchronous motor based on analysis of nonlinear inductance,". *Proceedings of the CSEE*, vol. 31, no. 30, pp. 69-76, 2011.

[7] A. Boduroglu, Y. Demir, B. Cumhur and M. Aydin, "A novel track structure of double-sided linear PM synchronous motor for low cost and high force density applications," *IEEE Transactions on Magnetics*, vol. 57, no. 2, pp. 1-5, 2021.

[8] Xia Jiakuan, Wang Chengyuan, Li Haodong, et al. "Study of end-effects analysis and NN compensation technique of linear motor for high precision NC machine," *Proceedings of the CSEE*, vol. 23, no. 8, 2003.

[9] Jang Seok Myeong, Lee Sung Ho. "Comparison of two types of PM linear synchronous servo and miniature motor with air-cored film coil," *IEEE Transactions on Magnetics*, vol. 38, no. 5, pp. 3264-3266, 2002.

[10] Liao, Z., J. Yue, and G. Lin. "Application research of HTS linear motor based on Halbach array in high-speed maglev system," *IEEE Transactions on Applied Superconductivity*, vol. 1, no. 1, pp. 99-105, 2021.

[11] Kou Bao Quan, Huang Xu Zhen, Wu Hong-xing, et al. "Thrust and thermal characteristics of electromagnetic launcher based on permanent magnet linear synchronous motors," *IEEE Transactions on Magnetics*, vol. 45, no. 1, pp. 358-362, 2009.

Zhentian Liu was born in Shijiazhuang, China in 1990. He received his Ph.D. degree in electrical engineering from the Naval University of Engineering, Wuhan, China, in 2019. In 2019, he joined the National Key Laboratory of Science and Technology on Vessel Integrated Power System, Naval Univ. of Engineering. His current research interests include electrical devices and machines, especially the design, molding, simulation, and control of linear motors.

Qiaopeng Zhou was born was born in Shaoyang, China in 2000. He is currently pursuing the Ph.D. degree in electrical engineering of Naval Univ. of Engineering. His research interest includes design and application of the liner motors.

Weichao Li was born in in 1982. He has joined the Naval University of Engineering, where he is currently a Professor and a Ph.D. Supervisor. His current research interests include electrical devices and machines, especially the design and control of the linear motors.